PNAS RESEARCH ARTICLE | BIOPHYSICS AND COMPUTATIONAL BIOLOGY ENGINEERING

The strawberry-derived permeation enhancer pelargonidin enables oral protein delivery

Nicholas G. Lamson[a], Katherine C. Fein[a], John P. Gleeson[a], Alexandra N. Newby[a], Sijie Xian[a], Kyle Cochran[a], Namit Chaudhary[a], Jilian R. Melamed[a], Rebecca L. Ball[a], Kanika Suri[a], Vishal Ahuja[a,b], Anna Zhang[a,b], Adrian Berger[a,b], Dmytro Kolodieznyi[c], Brigitte F. Schmidt[c], Gloria L. Silva[c], and Kathryn A. Whitehead[a,b,1]

Edited by Robert Langer, Massachusetts Institute of Technology, Cambridge, MA; received May 22, 2022; accepted July 13, 2022

Although patients generally prefer oral drug delivery to injections, low permeability of the gastrointestinal tract makes this method impossible for most biomacromolecules. One potential solution is codelivery of macromolecules, including therapeutic proteins or nucleic acids, with intestinal permeation enhancers; however, enhancer use has been limited clinically by modest efficacy and toxicity concerns surrounding long-term administration. Here, we hypothesized that plant-based foods, which are well tolerated by the gastrointestinal tract, may contain compounds that enable oral macromolecular absorption without causing adverse effects. Upon testing more than 100 fruits, vegetables, and herbs, we identified strawberry and its red pigment, pelargonidin, as potent, well-tolerated enhancers of intestinal permeability. In mice, an oral capsule formulation comprising pelargonidin and a 1 U/kg dose of insulin reduced blood glucose levels for over 4 h, with bioactivity exceeding 100% relative to subcutaneous injection. Effects were reversible within 2 h and associated with actin and tight junction rearrangement. Furthermore, daily dosing of mice with pelargonidin for 1 mo resulted in no detectable side effects, including weight loss, tissue damage, or inflammatory responses. These data suggest that pelargonidin is an exceptionally effective enhancer of oral protein uptake that may be safe for routine pharmaceutical use.

oral drug delivery | protein therapeutics | permeation enhancers

Significance

Millions of patients have reported skipping therapeutic injections due to needle phobia or pain, which leads to poorer disease outcomes. Although simple and painless oral administration of protein therapeutics would circumvent patient hesitancy and suffering, it has not been possible because the intestine is not permeable to macromolecules, including protein. Here, we demonstrate that the strawberry pigment pelargonidin reversibly permeabilizes the epithelial lining of the intestines and enables efficient oral protein delivery without inducing inflammation or tissue damage in mice.

Millions of patients are subjected daily to injections of single-dose therapeutics (e.g., vaccines) and chronic therapies (e.g., insulin). Unfortunately, the pain and inconvenience of injections leads to noncompliance. For example, 45 to 60% of diabetic patients report that they have intentionally skipped doses of their medication as a result of injection-associated dread (1, 2). This noncompliance results in poor disease control and long-term complications that exacerbate patient suffering and inflate healthcare costs (3). In contrast to injections, oral delivery is painless and convenient (4). Its development for protein and other macromolecular drugs would dramatically improve patient experience, compliance, and outcomes for a variety of diseases, including type 1 and 2 diabetes (1–3), cancer (5, 6), and cardiovascular disease (3).

Oral delivery of most proteins is not currently possible because the epithelial cell lining of the intestine inhibits macromolecular absorption into the bloodstream. Specifically, the epithelial cells are joined together by tight junction complexes that prevent the paracellular (between-the-cells) passage of any molecule greater than ~1 nm, or 600 Da, in size (7, 8). Although there are numerous strategies to enhance oral bioavailability of larger therapeutics (9, 10), the majority of clinical studies have used chemical permeation enhancers to widen the diffusion channels in the tight junctions and facilitate absorption of macromolecules (11) (Fig. 1*A*). Unfortunately, many such efforts have been thwarted by enhancer-caused cytotoxicity or structural damage to the intestines (12, 13). Because of this, oral delivery has been approved by the Food and Drug Administration for only a handful of peptide drugs, which are relatively small compared to proteins (14).

To address the urgent need for safe intestinal permeation enhancers, we investigated materials that we hypothesized would be nontoxic in the gastrointestinal tract: plant-derived foods. Foods contain thousands of compounds that are well-tolerated by intestinal cells and the body as a whole. Over millions of years, humans and plants have coevolved via mutualism: Plants provide a source of nutrition for humans, while humans disperse seeds through cultivation, harvest, preparation, and defecation (15). Given this cooperation, edible plants and their molecular building blocks typically do not induce toxic or immunogenic responses in the intestine. For example, plant cell drug encapsulation strategies have been well-tolerated following oral administration (16, 17), and many plant-derived compounds cause beneficial antiinflammatory, antimicrobial, or anticancer effects (18–20).

Author affiliations: [a]Department of Chemical Engineering, Carnegie Mellon University, Pittsburgh, PA, 15213; [b]Department of Biomedical Engineering, Carnegie Mellon University, Pittsburgh, PA, 15213; and [c]Department of Chemistry, Carnegie Mellon University, Pittsburgh, PA, 15213

Author contributions: N.G.L., B.F.S., G.L.S., and K.A.W. designed research; N.G.L., K.C.F., J.P.G., A.N.N., S.X., K.C., N.C., J.R.M., R.L.B., K.S., V.A., A.Z., A.B., D.K., and B.F.S. performed research; N.G.L., K.C.F., J.P.G., A.N.N., N.C., D.K., and B.F.S. analyzed data; and N.G.L. and K.A.W. wrote the paper.

Competing interest statement: K.A.W. and N.G.L. are inventors on Patent Cooperation Treaty (PCT) application PCT/US2019/027885 and US patent application US 2021/0113519 A1, which cover aspects of the technology presented here.

This article is a PNAS Direct Submission.

[1]To whom correspondence may be addressed. Email: kawhite@cmu.edu.

This article contains supporting information online at http://www.pnas.org/lookup/suppl/doi:10.1073/pnas.2207829119/-/DCSupplemental.

Published August 9, 2022.

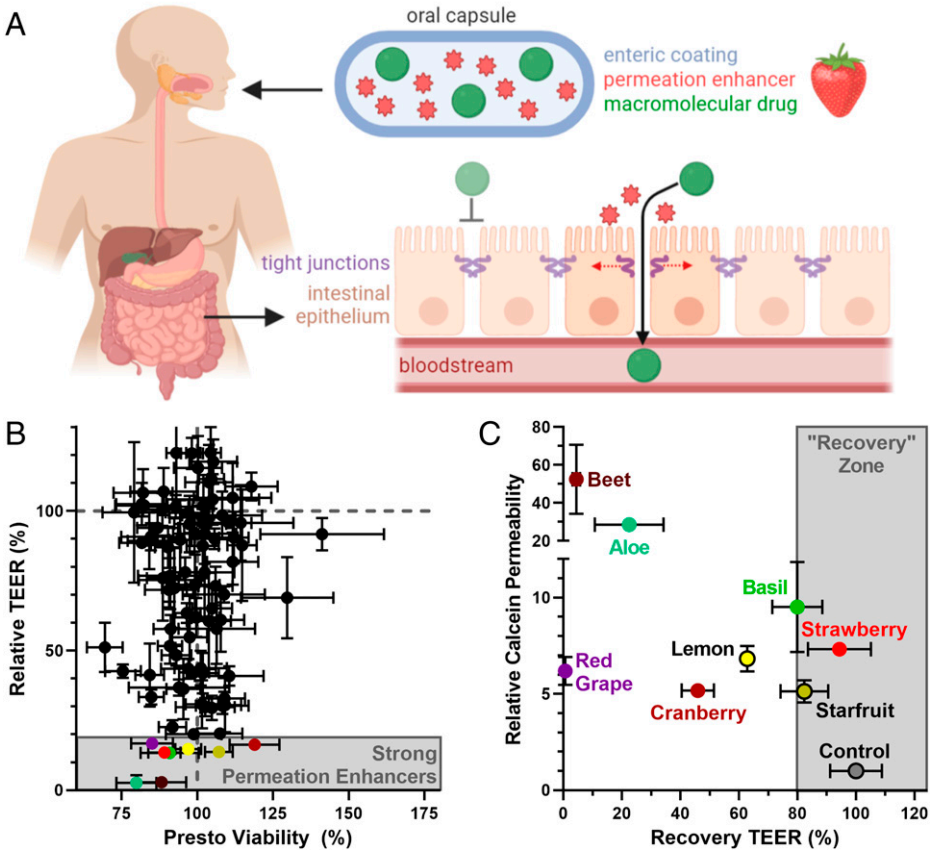

Fig. 1. Plant-derived foods are a novel source of nontoxic permeation enhancers that enable oral protein delivery. (*A*) A food-derived permeation enhancer is incorporated into a capsule containing a powdered macromolecular drug (e.g., insulin) for oral administration. The capsule is coated with a pH-sensitive polymer (enteric coating) that delays release of the enhancer and drug until the capsule has localized to the small intestine. There, the enhancer opens the tight junctions between intestinal cells, enabling the protein drug to enter circulation. (*B*) Food extracts screened at 15 mg/mL on Caco-2 cells exhibited a variety of behaviors, and well-tolerated food extracts differed in their effect on TEER (*y* axis), a surrogate measurement for intestinal permeability. Lower TEER typically corresponds to higher drug permeability. (*C*) The most effective TEER-reducing extracts increased the permeability of the model drug, calcein, across Caco-2 intestinal monolayers (*y* axis). Strawberry was chosen as our top candidate because it enabled full recovery of TEER values within 24 h of treatment removal (*x* axis). Error bars display SEM ($n = 3$ replicate wells for TEER and calcein permeability, $n = 8$ replicate wells for Presto viability).

Herein, we demonstrate that plant-derived foods contain numerous polyphenolic compounds that enhance intestinal permeability. Pelargonidin, an anthocyanidin derived from strawberry, was the most active of these compounds. When administered with the model protein insulin in an enteric coated capsule at a low dose of 1 U/kg, its resultant bioactivity was over 100% compared to subcutaneous injection. We also eliminated several safety concerns by showing that effects were rapidly reversible and that 1 mo of daily treatment with oral pelargonidin did not overpermeabilize the intestine, cause gross pathological changes, or provoke local or systemic inflammation.

Results and Discussion

To determine the suitability of plant-derived foods as intestinal permeation enhancers, we assembled a library of 106 fruits, vegetables, and herbs (*SI Appendix*, Table S1), collected primarily from grocery stores and farmer's markets or grown specifically for this study (e.g., otricoli orange berries). Each food was prepared by washing, removing inedible portions (e.g., peels or pits), and blending with deionized water to form a slurry. The slurry was then centrifuged and filtered to remove any water-insoluble materials, adjusted to neutral pH, and freeze-dried to yield a powdered extract. These extracts were dissolved at a concentration of 15 mg/mL, the upper concentration for uniform dissolution, in cell culture media for in vitro screening.

We first examined the hypothesis that food-derived compounds are nontoxic to intestinal cells. Specifically, extracts were incubated with Caco-2 intestinal cells for 3 h, then cell viability was measured using the PrestoBlue assay (*SI Appendix*, Table S1). As expected, most fruit, vegetable, and herb extracts did not statistically significantly reduce Caco-2 cell viability (*SI Appendix*, Fig. S1 and Fig. 1*B*). Those that did impact cell survival included garnishes and herbs that humans do not typically consume in large quantities (e.g., citrus rinds and rosemary). We also noted that several fruits known to contain protease enzymes (including kiwi, pineapple, and papaya) registered as cytotoxic according to the PrestoBlue assay. Visual inspection revealed that these extracts were not killing the cells but simply lifting them from the culture plate in the same manner that trypsin dissociates adherent cells during passaging.

We next took the noncytotoxic extracts and examined their permeation enhancement efficacy by measuring the transepithelial electrical resistance (TEER) of treated Caco-2 monolayers (21). TEER measures the resistance of the cell monolayers to ion passage, so a reduction in TEER indicates increased intestinal permeability (22, 23). Extracts produced a wide range of effects on permeability (Fig. 1*B*). While many extracts did not impact TEER (*y* axis values near the dashed gray line), a subset produced excellent permeation enhancement (TEER values less than 50%). Interestingly, a small number of extracts rendered the monolayers less permeable (e.g., raspberry; *SI Appendix*, Table S1), which may be useful in the context of leaky gut therapy (24).

For the most promising permeation-enhancing extracts (colored points in Fig. 1*B*), we confirmed that TEER reductions correspond with increased permeability. Specifically, we measured transport of the fluorescent molecule calcein, a 623-Da model drug, across Caco-2 monolayers (*y* axis, Fig. 1*C*). Because permeability of treated monolayers developed over time, typically taking 2 h to equilibrate, calcein transport data are expressed as a quasi-steady-state permeability relating the mass transported for 1 h before treatment addition to that transported between the 2- and 3-h posttreatment marks. As expected, the selected extracts increased calcein permeability. Improvements ranged from 5-fold (cranberry) to more than 50-fold (beet). Because reversibility is an important feature of a safe permeation enhancer, we also measured TEER 24 h after extract removal (*SI Appendix*, Table S1). All TEER data are displayed as percentage of the same monolayers' TEER values before treatment addition (*x* axis, Fig. 1*C*). We chose strawberry for future experiments because it offered the most promising combination of permeation enhancement and monolayer recovery.

Next, we focused on the most critical question for further technology development: Of the thousands of chemical compounds found in strawberry, which is responsible for strawberry's reversible and nontoxic permeabilization of the intestine? Our screening results revealed an intriguing trend: The effect of some fruits and vegetables varied dramatically as a function of color. For example, while red tomatoes, grapes, and potatoes were effective permeation enhancers, yellow tomatoes, green grapes, and white potatoes were not (Fig. 2*A*). Based on these data, we wondered whether our active, permeation-enhancing compound may be a pigmented molecule.

To test this theory, we grew a crop of the Carolina Pineberry, a white-fruited strawberry cultivar (Fig. 2*B*). When applied to Caco-2 monolayers, these white strawberries failed to enhance intestinal permeability (Fig. 2*C*), confirming that we were searching for a compound related to coloration. The most abundant class of pigmented compounds in strawberries is the polyphenols (25), defined by the presence of multiple phenol groups (26). Given that white strawberries have multiple down-regulated synthesis pathways for polyphenols (27), we next examined strawberry polyphenols as a narrowed set of potential permeation enhancers.

To isolate polyphenols, we ground freeze-dried strawberries to a powder, extracted them with ethanol, and dried the resulting material. We then dissolved this in methanol and applied it to Amberlite XAD7 resin, which selectively adsorbs phenol groups (28) (Fig. 2*D*). Vacuum filtration of the resin removed all the nonphenolic material with the methanol and subsequent water washes, and the polyphenols were eluted using ethanol. After drying, this separation process yielded ∼3.5 g of polyphenol extract per kilogram of strawberries (about 50 strawberries).

When applied to Caco-2 monolayers, the nonphenolic material did not affect permeability as measured by TEER (Fig. 2*E*). However, the polyphenols boosted calcein permeability to the same extent as the crude strawberry extract at only one-third the concentration (Fig. 2*F*). With a purer permeation enhancer in hand, we next asked whether our cell culture results extended in vivo. For initial experiments, we orally dosed mice with strawberry polyphenols and 4-kDa fluorescein isothiocyanate (FITC)-labeled dextran (FITC-DX4), which is a nondigestible and fluorescent macromolecule commonly used to model oral uptake of small proteins. As expected, the strawberry polyphenols more than doubled FITC-DX4 absorption across the intestinal barrier (Fig. 2*G*). We observed a similar increase in uptake for orally administered 40-kDa FITC-dextran (FITC-DX40) (Fig. 2*H*), suggesting that the strawberry polyphenols can be used to orally deliver midsized macromolecular drugs.

We then probed whether strawberry-derived polyphenols enable the oral delivery of a functional protein. As a proof of concept, we chose insulin (5.8 kDa) because 1) it is widely prescribed but not orally bioavailable and 2) its bioactivity is readily assessed from a drop of whole blood. Specifically, insulin enables sugar uptake into cells and results in lower blood glucose levels. In these experiments, mice received an oral dose of strawberry polyphenols, followed 1 h later by an injection of insulin directly into the small intestine to circumvent transit time and degradation in the stomach. Blood glucose levels for each mouse were monitored over 5 h and were normalized to the individual animal's reading immediately before insulin administration. Mice receiving insulin and strawberry polyphenols experienced a substantial and sustained reduction in blood glucose concentration compared to mice that received insulin after a saline gavage (Fig. 2*I*). Further, the strawberry polyphenols and intestinal insulin combination sustained hypoglycemia for at least 3 h longer than the same 1 U/kg dose of subcutaneous insulin, the current gold standard of administration.

Encouraged by these bioactivity data, we resumed our search for a single, active component of strawberry and turned to medium-pressure liquid chromatography (MPLC) for further resolution of the strawberry polyphenol extract (*SI Appendix*, Fig. S2). Briefly, the polyphenol mixture was separated by an initial MPLC run, and consecutive fractions were combined based on color and similarity of ultraperformance liquid chromatography (UPLC) traces. The pooled samples were further separated by four additional runs of MPLC and recombined based on UPLC traces. This yielded 22 fractions, including two pure compounds, for screening on Caco-2 monolayers. Although the vast majority of the samples did not affect epithelial permeability (Fig. 3*A*), one fraction, ε3, was an exceptional permeation enhancer. The late elution of ε3 from the columns identified it as one of the less hydrophilic members of the polyphenol family. It was also deep red in color and a very small fraction, yielding less than 3 mg from 1 g of polyphenol starting material. While the small quantity of product suggested that the fraction was particularly potent, it also complicated efforts to discern its molecular identity.

To expedite our identification of fraction ε3, we purchased a library of 27 known phenolic compounds from strawberry. As with the chromatography fractions, we screened these for their bioactivity on Caco-2 cells at 1 mg/mL concentration (Fig. 3*B*). Fortuitously, one of these compounds was an effective permeation enhancer: pelargonidin. Pelargonidin (Fig. 3*C*) and its glucoside, callistephin, contribute to the red coloration in strawberries (29), with the vast majority of the pigment present as glycoside (30). However, our screening showed that callistephin was not effective, and that only the aglycone form of pelargonidin improved epithelial permeability. This is consistent with the observation that the effective fraction, ε3, yielded a small mass of deep red, fairly hydrophobic material. We further confirmed the common identity of ε3 and pelargonidin by mass spectrometry (*SI Appendix*, Fig. S3) and NMR (*SI Appendix*, Fig. S4) and comparable activity on Caco-2 monolayers (*SI Appendix*, Fig. S5). Treatment of Caco-2 monolayers with commercially obtained pelargonidin led to dose-dependent reductions in TEER (Fig. 3*D*) and improvements in calcein permeability (Fig. 3*E*) without reducing cell viability (*SI Appendix*, Fig. S6).

We then asked whether commercially available pelargonidin, like strawberry extracts, enables oral macromolecule delivery in mice. First, we examined the kinetics of permeation enhancement

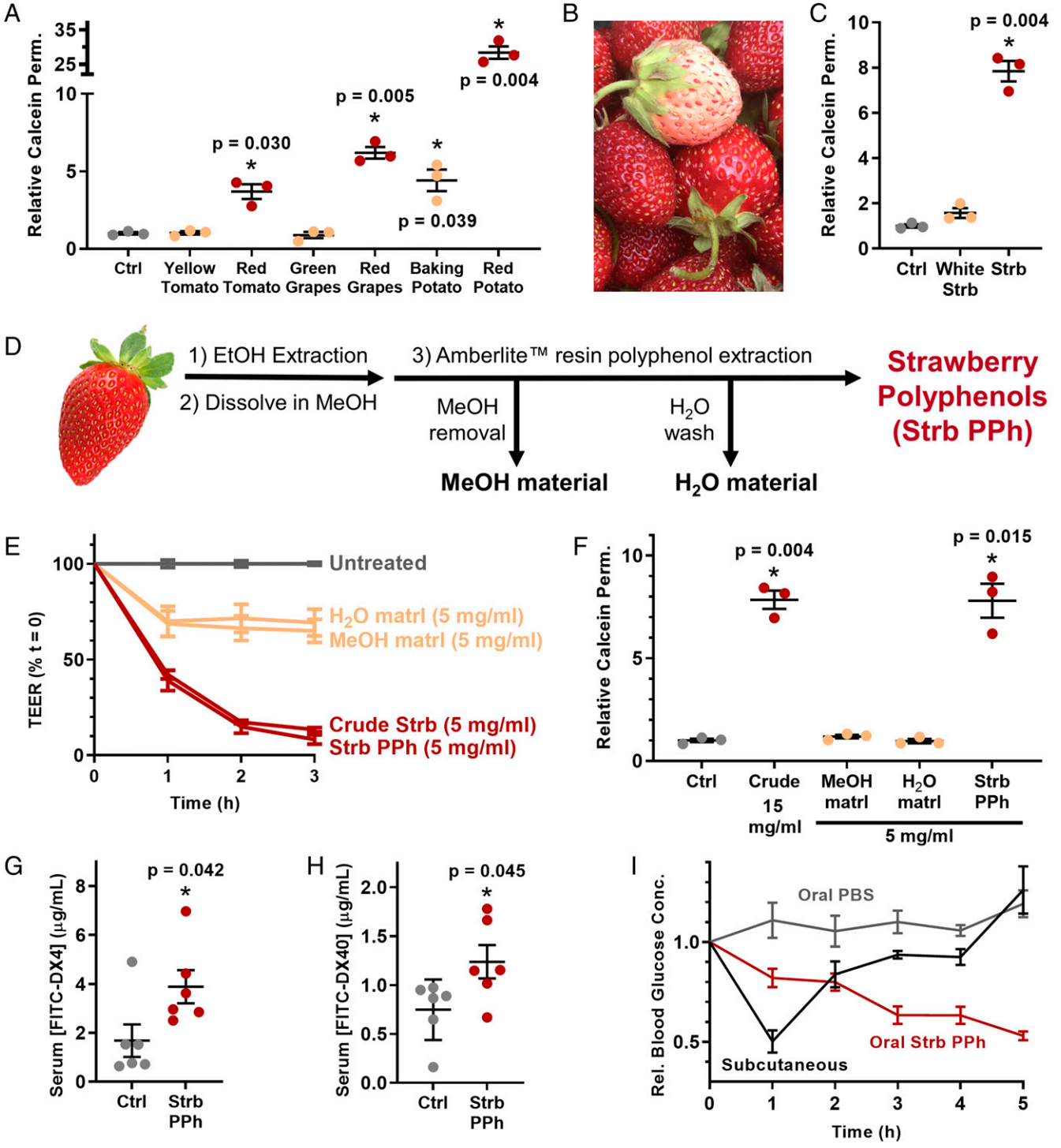

Fig. 2. Polyphenolic compound(s) in strawberry enhance intestinal permeability. (*A*) Only the red varieties of several foods enhanced the permeability of Caco-2 monolayers. (*B*) White Carolina Pineberry strawberries were grown for this study. (*C*) White strawberries, which lack polyphenolic pigments, were not effective permeation enhancers. (*D*) Polyphenols were extracted from strawberry via adsorption to Amberlite resin and a sequence of washing steps. (*E*) Polyphenolic compounds isolated from strawberries enhanced intestinal permeability by TEER and (*F*) by calcein permeability to the same extent as crude strawberry extract at one-third of the dose. (*G*) Treatment with strawberry polyphenols doubled the uptake of orally administered 4-kDa dextran (FITC-DX4) and (*H*) 40-kDa dextran (FITC-DX40) in mice. (*I*) One unit per kilogram of insulin was delivered by intestinal injection following oral delivery of either saline (control) or strawberry polyphenols and compared to subcutaneous injection of the same dose. Strawberry polyphenols induced sustained reductions in blood glucose levels. Integrated areas above the curves from *H* demonstrate that strawberry polyphenols enabled significantly better insulin bioactivity than subcutaneous injection. Error bars display SEM ($n = 3$ replicate wells for *A*, *C*, and *E*, $n = 6$ mice for panels *F* and *G*, and $n = 5$ mice for *H* and *I*). *$P < 0.05$ with respect to control by two-tailed t test with Welch's correction.

following oral pelargonidin treatment using FITC-DX4. Intestinal permeability was highest 1 h after treatment (Fig. 4*A*) and returned to phosphate-buffered saline (PBS)-treated control levels within an additional hour. These data suggest a swift reversibility of effect, assuaging the concern that permeation enhancers permit the unregulated transport of toxins over prolonged periods. Experiments focusing on size of drug cargoes showed that improved uptake of orally delivered 40-, 70-, and 150-kDa dextrans decreased with larger size (Fig. 4*B*). Such size-dependent transport suggests that pelargonidin would not allow for large

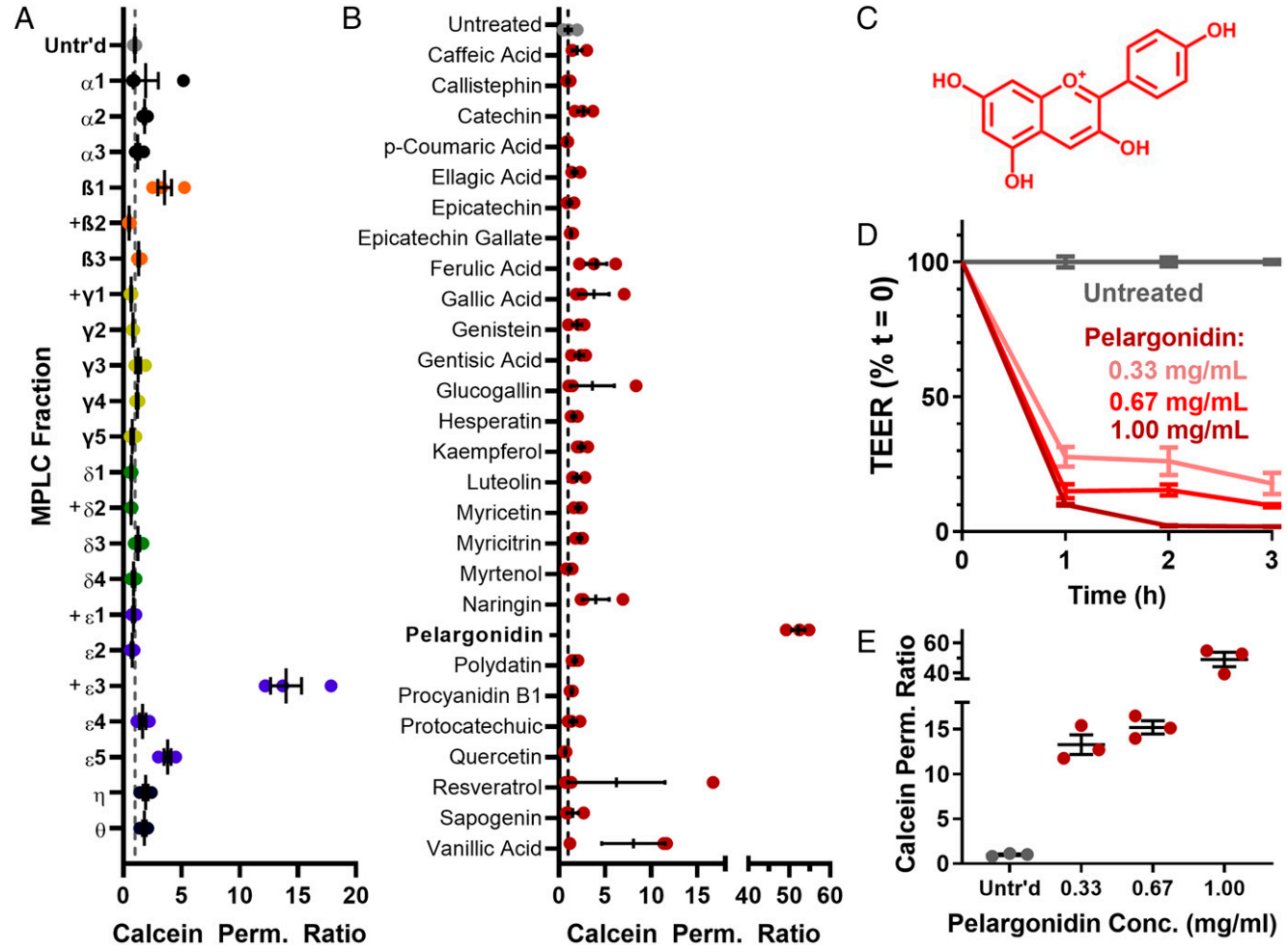

Fig. 3. Chromatographic separation of strawberry polyphenols identified pelargonidin as the primary, active permeation enhancer. (*A*) Of 22 fractions that resulted from MPLC separations of strawberry polyphenols, only the ε3 fraction enhanced the permeability of Caco-2 monolayers. "+" denotes fractions that were too small to examine at the otherwise standardized concentration of 1 mg/mL. (*B*) Similarly, of a large group of commercially purchased phenolic compounds known to occur in strawberries, only the pigment molecule pelargonidin significantly increased the permeability of calcein across cell monolayers. (*C*) Chemical structure of pelargonidin. (*D*) Pelargonidin permeabilized intestinal Caco-2 cells, as measured by TEER, and (*E*) improved calcein permeability in a dose-dependent manner. Error bars represent SEM (n = 3 or 4 replicate wells).

material, such as virus capsids or bacteria, to migrate out of the intestines and into the body. This property is critical for long-term tolerability of permeation enhancers and has likewise been demonstrated in the Transient Permeation Enhancer technology that has achieved recent clinical and commercial success for oral delivery of the small peptide octreotide (31, 32).

We again used insulin to demonstrate that pelargonidin enables the delivery of functional protein drugs across the intestinal barrier. Following oral pelargonidin administration, intestinal injections of insulin (1 U/kg) induced sustained decreases in blood glucose over at least 4 h, while a subcutaneous injection induced a pronounced but brief response (Fig. 4*C*). Area above the curve calculations showing that pharmacodynamic activity of intestinal insulin at the highest pelargonidin dose (80 mg/kg) is approximately double that of subcutaneous insulin (Fig. 4*D* and Table 1). This improves upon other promising, recently reported strategies for oral insulin delivery, including ionic liquid (33) and anionic nanoparticles (34), which achieve between 60% and 100% relative bioactivity.

Next, to demonstrate the efficacy of a fully oral delivery system, we loaded pelargonidin and insulin together into mouse-sized capsules and coated them with the enteric polymer Eudragit L100-55 to protect them from acid- and enzyme-mediated degradation in the stomach. When orally administered to mice, capsules containing insulin or pelargonidin alone did not demonstrate any pharmacodynamic difference compared to blank capsules (*SI Appendix*, Fig. S7). However, a combination of pelargonidin and an insulin dose of only 1 U/kg decreased blood glucose concentrations for at least 4 h (Fig. 4*E*). In contrast, a 1 U/kg subcutaneous injection of insulin produced a sharp hypoglycemic effect that resolved within 3 h. Area above the curve calculations determined that the insulin–pelargonidin capsules at 1 U/kg were twice as bioactive as subcutaneous insulin (Fig. 4*F*). To our knowledge, this is the highest oral insulin bioactivity reported in the literature. Mucoadhesive intestinal patches (35) and anionic nanoparticle permeation enhancers (34) in healthy animals have achieved 7% and 29% relative insulin bioactivity, whereas this system produces 140% of the pharmacodynamic potency per insulin molecule (Table 1). The oral dose of 1 U/kg insulin used here is an improvement upon the 10- to 100-U/kg doses required by other oral delivery systems (33–35).

Having demonstrated the unusual efficacy of pelargonidin as an intestinal permeation enhancer for oral protein delivery, we conducted mechanistic and toxicity experiments to evaluate potential for long-term use. First, we examined the rearrangement of tight junction proteins upon pelargonidin treatment in Caco-2 cells via immunofluorescence and confocal microscopy.

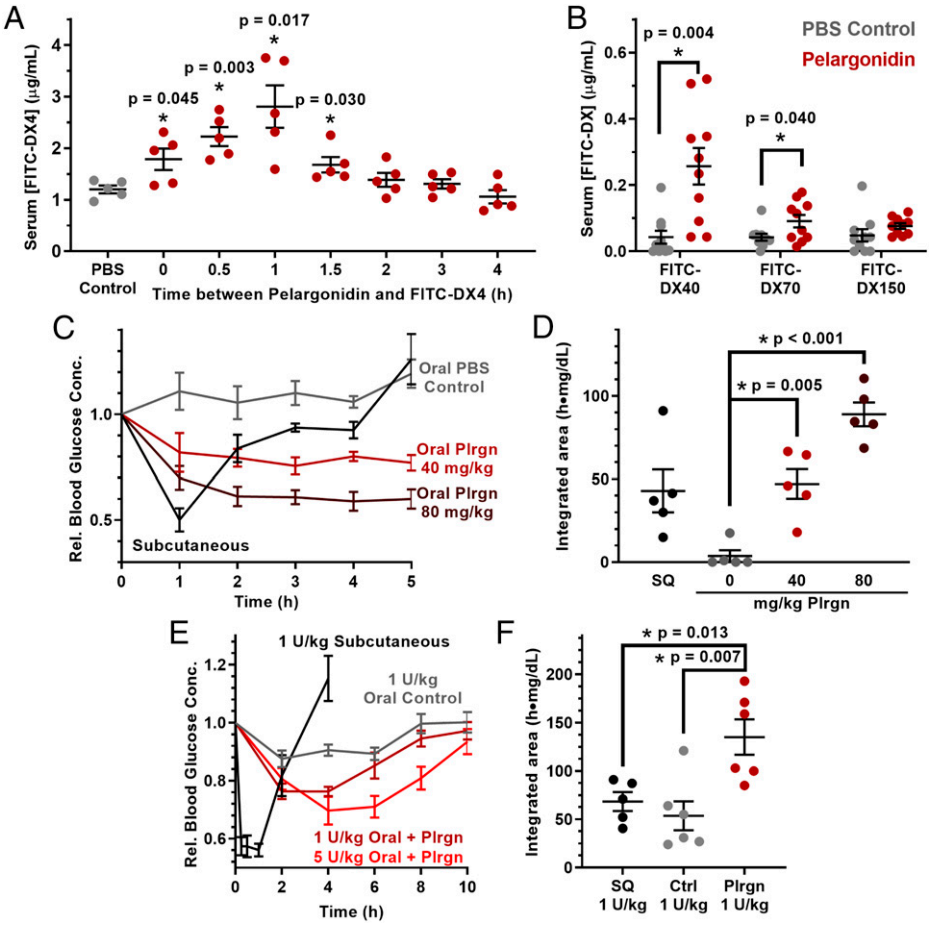

Fig. 4. Pelargonidin, the active component of strawberry, enables oral delivery of functional proteins in mice. (*A*) Kinetic experiments of pelargonidin permeation enhancement in mice showed that intestinal permeability to 4-kDa FITC-dextran (FITC-DX4) peaks 1 h after treatment and returns to baseline within another hour. (*B*) Pelargonidin treatment improved uptake of 40-kDa dextran but increased permeability tapered off for larger dextrans. (*C*) The efficacy of intestinally injected insulin at a dose of 1 U/kg was dependent on the dose of oral pelargonidin pretreatment, with (*D*) higher pelargonidin doses leading to higher bioactivity of the insulin. (*E*) Oral insulin doses of 1 U/kg (maroon) and 5 U/kg (red) reduced blood sugar in healthy mice when administered with pelargonidin in capsules. (*F*) Pelargonidin–insulin capsules resulted in double the bioactivity of subcutaneously injected insulin for 1 U/kg oral insulin. Error bars represent SEM (n = 8 to 10 mice for *B*, n = 5 or 6 for all other experiments). *P < 0.050 with respect to control, unless otherwise denoted, by two-tailed t test with Welch's correction.

While nuclear staining and midcell actin were consistent between untreated (Fig. 5*A*) and pelargonidin-treated cells (Fig. 5*B*), pelargonidin rearranged actin at the apical (luminal) cell surface (Fig. 5 *C* and *D*), which is in the vicinity of tight junctions (36). The junction anchoring protein, zonula occludens 1 (ZO-1) (Fig. 5 *E* and *F*), and the tight junction protein, occludin (Fig. 5 *G* and *H*), delocalized from the tight junctions and displayed large gaps in the normally continuous rings at the boundary of each cell. By pretreating Caco-2 monolayers with a collection of small-molecule enzyme inhibitors we determined that myosin light chain kinase (MLCK) is a critical mediator of pelargonidin-induced permeability (*SI Appendix*, Fig. S8). MLCK can remodel the actin cell skeleton (37) and has been shown to modulate the paracellular transport of insulin (38).

Table 1. Relative bioactivity values for insulin delivered with or without pelargonidin absorption enhancer in healthy mice

Delivery route	Insulin dose, U/kg	Pelargonidin, mg/kg	rBGmin, %	AAC, [(h·mg)/dL]/(U/kg)	rBA, %
SQ (5 h)	1	0	50.1 ± 5.5	42.9 ± 12.8	100.0
Intestinal (5 h)	1	0	100.0 ± 0.0	3.7 ± 3.5	8.7
	1	40	75.5 ± 4.0	47.1 ± 5.2	109.7
	1	80	58.9 ± 4.5	88.9 ± 7.1	207.2
SQ (10 h)	1	0	56.1 ± 2.2	68.5 ± 9.8	100.0
Oral (10 h)	1	0	87.6 ± 2.9	53.7 ± 15.4	(−9.8)
	1	40	76.3 ± 1.6	135.2 ± 18.2	140.2
	5	40	69.7 ± 4.9	152.0 ± 25.8	34.2
	0	40	86.4 ± 1.9	59.0 ± 8.2	0.0

Data are presented as arithmetic average ± SE (n = 5 or 6 mice for 5-h experiments and 8 to 10 mice for 10-h experiments). rBGmin = minimum average relative blood sugar achieved. AAC = insulin dose adjusted area above the blood glucose curve. rBA = dose-adjusted relative bioactivity. SQ = subcutaneous injection.

Inhibition of rho-associated protein kinase (ROCK) or kinase c-Src diminished but did not fully prevent the efficacy of pelargonidin. None of the other signaling enzymes that we examined proved necessary to the permeabilization process.

To address concerns that pelargonidin permeation-enhancing treatment may cause damage to intestinal mucosae (39), we performed a long-term safety experiment. Specifically, we orally dosed mice with 40 mg/kg pelargonidin every day for 30 d. Half of the animals were monitored for an additional, 7-d "recovery" period after treatment. In each case, we compared several intestinal and systemic health outcomes in pelargonidin-treated subjects to control animals receiving saline gavages. Treated mice did not lose weight during the study (Fig. 5*I*), nor did they experience elevated blood levels of the intestinal inflammation markers lipopolysaccharide binding protein (40) (LBP; Fig. 5*J*), intestinal fatty acid binding protein (41, 42) (I-FABP; Fig. 5*K*), or procalcitonin (42) (PCT; Fig. 5*L*). Further, gene expression analysis of mice's small intestinal epithelia revealed no significant changes in the expression of the pore-forming tight junction protein Claudin 2 (43) (CLDN2; Fig. 5*M*) or the barrier-forming proteins Claudin 3 (CLDN3; Fig. 5*N*), Zonula Occludens 1 (ZO-1; Fig. 5*O*), and Junctional Adhesion Molecule A (JAMA; Fig. 5*P*) (44).

Finally, we collected small intestine samples and stained them with hematoxylin and eosin for histological analysis. Comparison of duodenal tissue between control mice (Fig. 5*Q*) and pelargonidin-treated mice (Fig. 5*R*) revealed no immune cell invasion, necrosis, or discernible changes in tissue architecture. Similarly, there were no observable differences between proximal colon tissues from control (Fig. 5*S*) and pelargonidin-treated (Fig. 5*T*) animals. Taken together, these data indicate that daily intake of pelargonidin, at doses effective for oral drug delivery, is unlikely to cause intestinal or systemic toxicity.

Through this work we have demonstrated that pelargonidin, a red pigment abundant in strawberries, enables the oral administration of macromolecules from a standard, enteric-coated capsule. Pelargonidin reversibly permeabilized the gut without adverse effects following 1 mo of daily oral administration. Proof-of-concept delivery for proteins was established with low

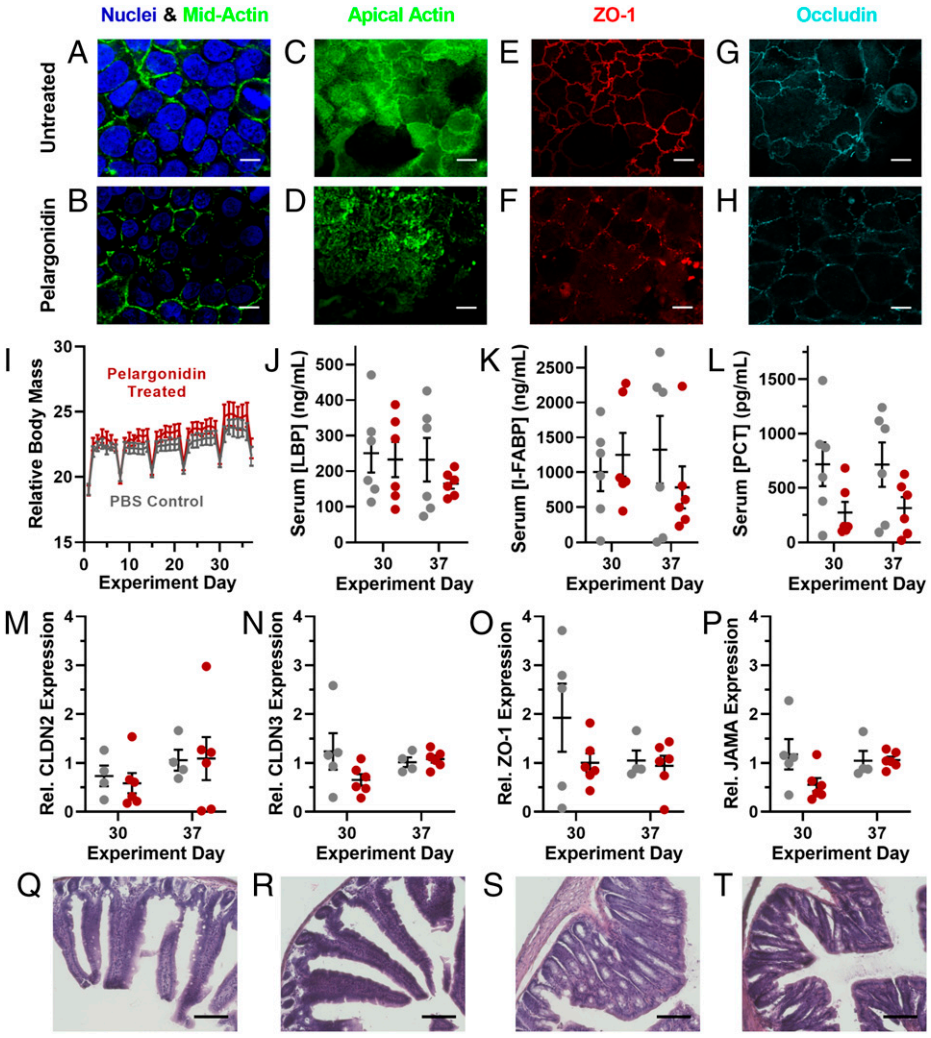

Fig. 5. Pelargonidin induces reversible, nontoxic opening of intestinal tight junctions. (*A*) Compared to untreated Caco-2 cells, (*B*) pelargonidin-treated monolayers showed no difference in morphology for nuclei or midcell actin. (*C* and *D*) However, actin at the apical surface, as well as the tight junction proteins (*E* and *F*) ZO-1 and (*G* and *H*) occludin rearranged into more punctate forms as a result of pelargonidin treatment. (*I*) During 1 mo of daily pelargonidin treatment, mice did not lose weight compared to control animals. Periodic weight loss was observed in both control and treated groups as a result of overnight fasting for weekly checkups. (*J*) Treated mice did not develop elevated levels of the inflammation markers LBP, (*K*) I-FABP, or (*L*) PCT. qRT-PCR revealed no statistical difference in mRNA expression of the tight junction proteins (*M*) Claudin 2, (*N*) Claudin 3, (*O*) ZO-1, or (*P*) JAMA in the small intestines of control and pelargonidin-treated mice. (*Q*) Representative histological images of duodenal sections of the small intestines from control mice and (*R*) pelargonidin-treated mice displayed no tissue damage resulting from treatment. (*S*) There were also no discernable histological differences between proximal colon samples from control and (*T*) treated mice. (White scale bars, 10 μm; black scale bars, 100 μm.) Error bars represent SEM (n = 4 to 12). For *I*–*P*, no comparisons between treated and control mice achieved statistical significance by two-tailed t test with Welch's correction.

doses of insulin, and dextran absorption highlighted the potential for extension to biopharmaceutical agents of differing size, structure, and composition. This versatility, combined with its unusual efficacy, suggests that pelargonidin and other fruit-derived permeation enhancers may provide a new solution to the clinical challenge of oral macromolecule delivery.

Materials and Methods

Materials. Penicillin/streptomycin, trypsin–ethylenediaminetetraacetic acid (trypsin-EDTA), PBS, fetal bovine serum (FBS), rat tail Collagen I, PrestoBlue viability kits, Hoechst 33342, calcein, DAPI, AlexaFluor 488-conjugated phalloidin, AlexaFluor 594-conjugated Anti-ZO-1 antibodies, and AlexaFluor 594 Anti-Occludin antibodies were purchased from Life Technologies (Thermo Fisher subsidiary). Caco-2 cells were purchased from American Type Culture Collection (ATCC). Dulbecco's modified Eagle's medium (DMEM), Amphotericin B, Falcon 225-cm^2 tissue culture flasks, Falcon HTS 24-Multiwell Insert Systems with 1-μm pores, Falcon 24-well plates, Corning CellBIND 96-well microplates, sodium butyrate, MITO+ serum extender, Whatman filter paper, Aimstrip Plus blood glucose strips, blood glucose monitor, gentisic acid, furoic acid, ellagic acid, kaempferol, naringin, vanillic acid, protocatechuic acid, ferulic acid, caffeic acid, lactone hexose, resveratrol, luteolin, bovine serum albumin (BSA), and optimal cutting temperature (OCT) mounting media were obtained from VWR. FITC-labeled dextrans (neutral charge, FD product line), Amberlite XAD7 resin, recombinant human insulin, aprotinin, catechin, epicatechin, polydatin, myricitrin, myricetin, hesperetin, myrtenol, gallic acid, metoclopramide hydrochloride, streptozotocin, U-73122, SR 3677, PP2, API-1, AZ 628, PIK, Harris modified hematoxylin, and alcoholic eosin Y were purchased from Sigma-Aldrich. C18 bulk silica gel SMT-Bod-C18 was purchased from Separation Methods Technologies. Callistephin and procyanidin B1 were obtained from Alkemist Labs. Epicatechin gallate and pelargonidin were from ChromaDex. Genistein, glucogallin, and sarsasapogenin were purchased from Toronto Research Chemicals. Mouse-sized (M) capsules and dosing kit were supplied by Torpac and Eudragit L100-55 enteric coating polymers were a gift from Evonik. DMSO-d_6 and tetramethylsilane (TMS) were purchased from Cambridge Isotope Laboratories. The complementary DNA (cDNA) reverse transcriptase kit; primers for Beta-Actin, ZO-1, Claudin-2, Claudin-3, and JAM-A; and SYBR Select Master Mix were ordered from Applied Biosystems. Enzyme-linked immunosorbent assay (ELISA) kits PCT, LBP, and fatty acid binding protein 2 (I-FABP) were purchased from Abclonal.

Preparation of Crude Food Extract Library. Food samples were obtained from local supermarkets and farmer's markets or grown from nursery seed/stock (Baker Creek Heirloom Seeds, Stark Bro's Nurseries and Orchards Co.) in K.A.W.'s garden (Pittsburgh, PA), totaling 106 fruits, vegetables, and herbs (*SI Appendix*, Table S1). After removing inedible portions (e.g., seeds and stems), the samples were blended with 125% wt/wt distilled water on medium-high speed for 3 min using a household blender. The resulting slurry was transferred to 50-mL conical tubes and centrifuged for 30 min at 400 rcf and room temperature. The resulting liquid was centrifuged to remove insoluble components, and the supernatant filtered through standard coffee filters to remove any large particulate matter, isolating water-soluble components that are compatible with aqueous cell culture assays. The extracts were then adjusted to neutral pH (7) with 1 M NaOH, and lyophilized. The resulting powders were stored at −80 °C until use, when they were dissolved at 15 mg/mL in cell culture media immediately before testing.

Cell Culture. Caco-2 lines were confirmed mycoplasma-free by direct DNA staining with Hoechst 3334229. Cells were cultured in DMEM supplemented with 10% FBS, 100 IU/mL of penicillin, 0.1 mg/mL streptomycin, and 0.25 μg/mL Amphotericin B ("Caco-2 media"). Cultures were incubated at 37 °C in a fully humid, 5% CO_2 environment. The cells were subcultured with 0.25% trypsin-EDTA and subsequent passaging every 3 to 4 d at ratios between 1:3 and 1:8. Cells at passage numbers 20 to 50 were utilized for further experiments.

PrestoBlue Assay. Caco-2 cells were seeded in a clear-bottom, black, 96-well plate at a concentration of 10^4 cells per well. After incubating the plate overnight at 37 °C, the media in the wells was aspirated and replaced with the treatment solutions (15 mg/mL for crude extracts or reported concentrations for pelargonidin, 100 μL/well). Sets of cell-free wells were also given extract treatments to ensure that food compounds did not interfere with the assay. After 3 h of exposure, the treatments were aspirated. PrestoBlue reagent (10 μL/well) and Caco-2 media (90 μL/well) were added to the wells. Thirty minutes later, a BioTek Synergy2 automated plate reader was used to measure the fluorescent signal produced by viable cells. The viability of each treatment is expressed as the ratio of the fluorescence intensity of the treated cells (treated cell wells minus signal from treatments in cell-free wells) to that of the untreated cells.

Caco-2 Permeability Experiments. For TEER and diffusion marker permeability experiments, TRIM models of rapid, 3-d Caco-2 intestinal epithelial monolayers were employed (21). Briefly, Caco-2 cells were suspended in DMEM supplemented with MITO+ serum extender (basal seeding medium), seeded at a density of 2×10^5 cells per well on collagen-coated transwell membrane supports, and incubated for 24 to 48 h. The media was then changed to DMEM supplemented with MITO+ and 2 mM sodium butyrate (enterocyte differentiation medium, EDM) and incubated for 48 h. The TEER was monitored to confirm proper barrier formation, and only monolayers with initial TEER values of at least 150 $\Omega \cdot cm^2$ were utilized for TEER or molecular permeability experiments.

Transwell inserts containing Caco-2 monolayers were transferred to 24-well plates containing 1 mL DMEM per well and allowed to equilibrate for 30 min before recording initial resistance values using a Millicell voltohmmeter. Treatments were suspended in EDM (15 mg/mL unless otherwise specified) and applied to the apical chambers, and negative control wells received fresh EDM. For some batches of pelargonidin, predissolution in ethanol was required; in these cases, the controls were likewise adjusted to contain the same ethanol content as the treatments (<1%). TEER readings were taken after 15, 30, 60, 120, and 180 min. After 180 min, treatments were removed and the monolayers rinsed once with warm PBS before returning to for a 24-h recovery period.

For molecular permeability, calcein was applied at 0.5 mM into the apical side of the monolayers with the fruit treatments. After 1 h, media in the basal chambers was sampled and examined for fluorescence at 495/515 nm using the plate reader. Application of calibration curves yielded the amount of marker transferred across each monolayer, which was used in a quasi-steady-state approximation to the apparent permeability equation:

$$P_{app} = \frac{\Delta M}{C_a A \Delta t}, \quad [1]$$

where P_{app} is the apparent permeability through the monolayer, ΔM is the amount of calcein in the basal compartment, C_a is the apical calcein concentration, A is the monolayer area, and Δt is the time between samples. Permeability measurements are expressed as the ratio of each monolayer's permeability at 3 h of treatment to its permeability before treatment, normalized to any change in untreated control monolayers during that time.

Amberlite Separation of Strawberry Extracts. Polyphenols were isolated via a previously published method (28). Briefly, a strawberry extract produced by extracting lyophilized fruit with ethanol then drying via rotary evaporation and lyophilization. The material was dissolved in methanol and adsorbed onto Amberlite XAD 7 HP (acrylate ester) resin. The methanol was removed from the resin using a Buchner funnel and Whatman #11 filter paper and evaporated to dryness, yielding unabsorbed material, which comprises a wide variety of compounds. The beads were then washed with water, which was collected and lyophilized to produce a sample composed primarily of sugars and organic acids. Next, the beads were washed with ethanol to collect the remainder of the adsorbed material. The ethanol was removed via rotary evaporation, and any remaining water was lyophilized away to yield a solid, powdered polyphenol extract.

Chromatography. MPLC was performed using a Buchi Sepacore system. Glass columns were hand-packed with reverse-phase (C18) silica gel and each run utilized a gradient from 10 to 100% acetonitrile in water with 0.1% trifluoroacetic acid (TFA). Run α was implemented for a coarse separation of the strawberry polyphenol extract (*SI Appendix*, Table S2). Eluent absorption at 280 nm was monitored to track phenol group migration. Fractions were collected, concentrated via rotary evaporation, and reapplied to a longer, narrower column for runs β, γ, δ, and ε. Fractions were collected and reconcentrated for testing in cell culture.

Each MPLC fraction was analyzed by UPLC using a Waters Acquity UPLC system and Acquity UPLC C18 Column. Each run began with a 10-μL injection of concentrated MPLC eluent. The samples were separated with a linear gradient of 10 to 100% acetonitrile in water/0.1% TFA over 6 min (*SI Appendix*, Table S2). The eluent was monitored by a photodiode array detector, allowing each sample to be recorded for both the 280-nm absorbance trace over time and absorbance spectra of characteristic polyphenol peaks.

To obtain a larger quantity of fraction ε3 for characterization, a larger amount of strawberry polyphenol material (6.4 g) was used. This material was dissolved in 60 mL of [67% ethanol, 33% water with 0.1% TFA], sonicated for 5 min, and centrifuged at 300 × *g* for 4 min to remove any undissolved matter. The supernatant was reduced to 20 mL by rotary evaporation and applied to a 36- × 920-mm column hand-packed with reverse-phase (C18) silica gel. This column was run with the same solvent gradient as run α, at 50 mL/min. The corresponding fractions were confirmed via UPLC, concentrated, and subjected to the same conditions as the initial run ε, yielding ∼7 mg of sample. Before characterizing, the activity of the sample was confirmed on Caco-2 monolayers (*SI Appendix*, Fig. S5).

Mass Spectrometry. High-resolution mass spectra were obtained on a Thermo Scientific Exactive Plus EMR Orbitrap Mass Spectrometer (ThermoFisher Scientific). The electrospray ionization source was operated in the positive mode with spray voltage of 2.5 kV and ion transfer tube temperature at 270 °C. Gas flow was set to defaults for the used 10-μL/min injection which was performed using the syringe pump. Each scan consisted of three microscans with a detection range set over a mass range of 150 to 2,000 *m/z*.

NMR. ^{1}H and ^{13}C NMR spectra were recorded with a Bruker Avance 500 spectrometer using 3-mm tubes with DMSO-d_6 as solvent and TMS as an internal standard. ^{1}H and ^{13}C NMR were performed at 500 and 126 MHz, respectively, and chemical shifts are given as δ values.

Mouse Studies. All mouse experiments were approved by the institutional animal care and use committee (IACUC) at Carnegie Mellon University (Pittsburgh, PA) under protocol number PROTO201600017 and were performed in accordance with all institutional, local, and federal regulations. C57BL/6 mice were either purchased from Charles River Laboratories or obtained from an institutionally managed breeding colony. Prior to experiments, mice were housed in cages of no more than six animals, with controlled temperature (25 °C), 12-h light–dark cycles, and free access to food and water. Mice utilized in this study were female and 8 to 16 wk (dextran, intestinal insulin, and toxicity: 18- to 24-g weight range) or 24 to 30 wk old (protein drug capsules: 30- to 45-g weight range to ensure capsule passage through the gastrointestinal tract). Only mice within 6 wk of age were directly compared to one another (placed on the same graph) for consistency. The free-to-use PS power calculator (Vanderbilt) was used to determine the minimal sample size for which statistical power was greater than or equal to 0.8 (generally, $n = 5$ or 6), and individuals were only excluded from data collection if they expired in the middle of surgical procedures or the monitoring period. Mice were fasted 8 to 12 h the night before an experiment to limit the variability caused by food matter and feces in the gastrointestinal tract. Fasting also served to stabilize the animals' blood sugar for insulin activity experiments, with a starting blood glucose range of ∼70 to 120 mg/dL. Oral gavages were administered at a volume of 10 mL solution per kg of mouse body weight (10 μL/g). Intestinal and subcutaneous injections were administered at a volume of 1 mL/kg (1 μL/g).

Intestinal Permeability to Dextrans. For dextran efficacy studies, fasted mice were orally gavaged with treatment solutions (600 mg/kg STRB PPh or 40 mg/kg pelargonidin) then gavaged 1 h later with 600 mg/kg FITC-DX4. For some batches of pelargonidin, predissolution in ethanol was required; in these cases, the controls were likewise adjusted to contain the same ethanol content as the treatments (<1%). Three hours after the dextran gavage, blood was collected and centrifuged. The serum was removed and examined for FITC concentration by reading for fluorescence on the plate reader and comparing to a unique calibration curve for each experiment. For larger macromolecule studies, 40-kDa dextran (FITC-DX40), 70-kDa dextran (FITC-DX70), or 150-kDa dextran (FITC-DX150) was substituted at the same 600-mg/kg dose.

Intestinal Insulin Delivery. Following 10 h of fasting, mice were orally gavaged with PBS (for control) or strawberry treatments (600 mg/kg STRB PPh or 40 mg/kg pelargonidin). One hour later, their initial blood sugar was measured and the animals were placed under anesthesia. Their intestines were surgically exposed, and insulin was injected at the predetermined dose (1 unit insulin per kg body weight, unless otherwise specified) into the duodenum. Mice in the subcutaneous insulin injection group received an oral gavage of PBS and did not undergo surgical access to the intestines. The mice were closed and secured with tissue adhesive then kept under anesthesia as their blood sugar levels were monitored each hour for 5 h. An endpoint at 5 h was enforced for all experiments, as the combined effects of the anesthesia, dehydration, and reduced blood sugar prevented reliable survival beyond that point. For comparison to the current standard of insulin delivery, subcutaneous injections were given at 1 U/kg to additional mice, into the scruff on their necks. To determine areas above the curve (AAC) for each mouse, trapezoidal integration was used to sum the area between known points on the blood glucose curve and the starting blood glucose value for the individual animal. In the AAC calculations, mice returning above 100% of their starting blood glucose did not incur "negative area."

Capsule Preparation. Dry capsule contents were produced by combining insulin at the prescribed dose, the protease inhibitor aprotinin (25% capsule filling by mass, 25 mg/kg), pelargonidin if required (40% capsule filling by mass, 40 mg/kg), and inactive BSA filler then mixing thoroughly. Size M capsules were filled with 3 to 4 mg of the drug mixture and their exact weights recorded. Each capsule was then dip-coated three times in a 7% (wt/vol in ethanol) solution of Eudragit L100-55, drying completely under gentle airflow following each coat. The total dry weight of polymer added to each capsule ranged from 0.4 to 0.8 mg.

Oral Insulin Delivery with Capsules. Following a 10-h fasting period, large (>30 g) mice were checked for baseline blood glucose levels then injected subcutaneously with 5 mg/kg metoclopramide hydrochloride (to stimulate gastric emptying) and orally administered capsules. Capsules were chosen so small variations in filler weight matched small variations in mouse weight, giving insulin doses within 10% of the designated average dose. The capsules were immediately flushed into the stomach with a 200-μL gavage of PBS. Blood glucose was measured every 2 h for a total of 10 h and normalized to each mouse's reading before capsule administration. From the blood glucose measurements, AACs were calculated as previously described. These areas were used to calculate dose-corrected relative bioactivity as follows:

$$\textit{Relative Bioactivity} = \left(\frac{\beta\,\frac{U}{kg}\ AAC - 0\,\frac{U}{kg}\ Capsule\ AAC}{\beta\,\frac{U}{kg}}\right) \Big/ \left(\frac{1\,\frac{U}{kg}\ SQ\ AAC - 0\,\frac{U}{kg}\ SQ\ AAC}{1\,\frac{U}{kg}}\right) \times 100\%, \quad [2]$$

where β is the insulin dose in units per kilogram of the capsule treatment being examined and *SQ* is subcutaneous injection.

Confocal Microscopy. Monolayers were rinsed with PBS to remove treatments and fixed in 4% paraformaldehyde for 10 min. After being rinsed three times with PBS, they were permeabilized with 0.2% Triton X-100 for 10 min, rinsed three times with PBS, and blocked with 0.2% BSA solution for 30 min to limit nonspecific antibody binding then incubated for 1 h with staining solutions. The staining solution contained DAPI (12 μg/mL, 358 nm/461 nm) to mark nucleic acids, AlexaFluor 488-conjugated phalloidin (5 U/mL, 495 nm/518 nm) to bind actin, and AlexaFluor 594-conjugated Anti-ZO-1 (clone ZO1-1A12) antibodies or Anti-Occludin (clone OC-3F10) antibodies (50 μg/mL, 590 nm/617 nm) in 0.2% BSA. After staining, the monolayers were mounted on slides using ClearMount solution (Invitrogen) and sealed under coverslips using clear nail polish.

Prepared slides were imaged at 63× magnification using a Zeiss LSM 700 confocal microscope with ZEN 2012 SP1 software. Images were captured using a Plan-Apochromat 63×/1.40 oil DIC objective and an X-Cite Series 120Q laser source exposing at 405, 488, and 555 nm. Images were ∼101.5 μm × 101.5 μm and were captured with a lateral resolution of ∼0.3 μm. No additional processing or averaging was performed to enhance the resolution of the images.

ImageJ (NIH) image processing software was used to prepare confocal images for publication. Upper and lower thresholds were narrowed slightly to remove background noise and improve visibility of the signals. All images were

processed with the same thresholds and display lookup tables, which were linear throughout their ranges. Images were converted from their original 16-bit format to RGB color for saving and arrangement into figures. No other manipulations were performed.

Cell Signaling Inhibition. Caco-2 monolayers were incubated for an hour before treatment with small-molecule inhibitors, then pelargonidin was added without changing the inhibitor concentration. All changes in permeability were normalized to monolayers treated with the inhibitors but no pelargonidin. The inhibitors used were 10 μM FRAX 486 (p21-Activated Kinase, PAK, inhibitor), 10 μM U-73122 (Phospholipase C, PLC, inhibitor) 1 μM SR 3677 (Rho Kinase, ROCK, inhibitor), 1 μM PP2 (c-Src inhibitor), 100 μM API-1 (Protein Kinase B, Akt, inhibitor), 2 μM AZ 628 (Rapidly Accelerated Fibrosarcoma Kinase, Raf, inhibitor), or 0.33 mM PIK (Myosin Light Chain Kinase, MLCK, inhibitor).

Long-Term Safety Study. Cohorts of 12 mice each were treated for 30 d with oral pelargonidin (40 mg/kg) or PBS (negative control). Mice were weighed each day before oral gavages to ensure proper dosing. On day 31, half of the mice were killed and tissue and serum collected for later analysis. The remaining six mice per group were left untreated for an additional 7 d to assess their recovery from any cumulative effects of the pelargonidin treatment. Reported weights are normalized to the starting weight of the individual mouse and to the untreated control mice.

To determine levels of circulating cytokines and inflammatory markers, blood samples were separated via centrifugation. The serum was subjected to ELISA analysis per the instructions of the kit manufacturer.

For intestinal tight junction expression, tissue samples (1 cm) were collected from treated mice and homogenized in 0.5 mL TRIzol reagent using the Bead-Bug microtube homogenizer. Chloroform (0.1 mL) was added and centrifuged at 12,000 rpm for 15 min. The aqueous layer was removed and mixed with an equal volume of 100% ethanol, and the RNA was extracted with RNeasy mini kit (Qiagen) according to the manufacturer's instructions. cDNA was generated from 2,000 ng of RNA using High-Capacity cDNA Reverse Transcription Kit (Applied Biosystems). Quantitative real-time PCR (qRT-PCR) was performed using SYBR Select Master Mix (Applied Biosystems) on a ViiA 7 Real-Time PCR system (Applied Biosystems) and the primer sequences displayed in *SI Appendix*, Table S3. The expression of each messenger RNA (mRNA) was normalized to expression of the housekeeping gene Beta Actin and expressed as $R = 2^{-\Delta\Delta}$ct values.

Histology. Immediately following killing, mice from the safety study were dissected to collect their small intestines and colons. The organs were fixed in 4% formaldehyde for 24 h and transferred into 30% sucrose solution overnight at 4 °C. Sampled were embedded in OCT, and cross-sections of 10 μm were cut using a cryostat. Sections ere rinsed with PBS and stained in Harris hematoxylin for 8 min then washed twice in deionized water, differentiated for 1 min in 5% acetic acid, and washed with water two more times. The hematoxylin was blued using Scott's tap water (0.2% sodium bicarbonate and 1% magnesium sulfate at pH 8 in water) and washed twice more with water. The slides were stained in alcoholic eosin for 2 min then dehydrated with 95% and 100% ethanol before they were cleared in xylenes. The slides were mounted and allowed to dry in a fume hood overnight then imaged using an EVOS FL Auto 2 microscope (Thermo Fisher Scientific) at 20× magnification.

Statistics. All data presented as arithmetic mean of the given "*n*" number of replicates (individual animals or number of in vitro cell culture wells) and error bars display the SEM. For statistical significance markings, two-tailed Student's *t* tests with Welch's correction were used to calculate *P* values, which are displayed alongside the data.

Data, Materials, and Software Availability. All study data are included in the article and/or *SI Appendix*.

ACKNOWLEDGMENTS. We thank Lynn Walker for her advice and for supplying quinces from her home garden. This work was supported by NIH grant DP2-HD098860, NSF grant 1807983, the Wadhwani Foundation, and the Berkman Faculty Development Fund. N.G.L. acknowledges funding support from the Thomas and Adrienne Klopack Graduate Fellowship and NSF Graduate Research Fellowship Program (GRFP). This material is based on work supported by the NSF GRFP under grant DGE1252522. Any opinions, findings and conclusions or recommendations expressed in this material are those of the authors and do not necessarily reflect the views of the NSF.

1. M. Peyrot, R. R. Rubin, D. F. Kruger, L. B. Travis, Correlates of insulin injection omission. *Diabetes Care* **33**, 240–245 (2010).
2. A. Zambanini, R. B. Newson, M. Maisey, M. D. Feher, Injection related anxiety in insulin-treated diabetes. *Diabetes Res. Clin. Pract.* **46**, 239–246 (1999).
3. M. C. Roebuck, J. N. Liberman, M. Gemmill-Toyama, T. A. Brennan, Medication adherence leads to lower health care use and costs despite increased drug spending. *Health Aff. (Millwood)* **30**, 91–99 (2011).
4. E. Moroz, S. Matoori, J. C. Leroux, Oral delivery of macromolecular drugs: Where we are after almost 100 years of attempts. *Adv. Drug Deliv. Rev.* **101**, 108–121 (2016).
5. G. L. Banna *et al.*, Anticancer oral therapy: Emerging related issues. *Cancer Treat. Rev.* **36**, 595–605 (2010).
6. X. Du *et al.*, Current development in the formulations of non-injection administration of paclitaxel. *Int. J. Pharm.* **542**, 242–252 (2018).
7. L. Shen, C. R. Weber, D. R. Raleigh, D. Yu, J. R. Turner, Tight junction pore and leak pathways: A dynamic duo. *Annu. Rev. Physiol.* **73**, 283–309 (2011).
8. M. A. Navia, P. R. Chaturvedi, Design principles for orally bioavailable drugs. *Drug Discov. Today* **1**, 179–189 (1996).
9. A. Abramson *et al.*, An ingestible self-orienting system for oral delivery of macromolecules. *Science* **363**, 611–615 (2019).
10. A. M. Lowman, M. Morishita, M. Kajita, T. Nagai, N. A. Peppas, Oral delivery of insulin using pH-responsive complexation gels. *J. Pharm. Sci.* **88**, 933–937 (1999).
11. S. Maher, R. J. Mrsny, D. J. Brayden, Intestinal permeation enhancers for oral peptide delivery. *Adv. Drug Deliv. Rev.* **106** (Pt B), 277–319 (2016).
12. K. C. Fein, N. G. Lamson, K. A. Whitehead, Structure-function analysis of phenylpiperazine derivatives as intestinal permeation enhancers. *Pharm. Res.* **34**, 1320–1329 (2017).
13. S. Maher *et al.*, Evaluation of intestinal absorption enhancement and local mucosal toxicity of two promoters. I. Studies in isolated rat and human colonic mucosae. *Eur. J. Pharm. Sci.* **38**, 291–300 (2009).
14. T. D. Brown, K. A. Whitehead, S. Mitragotri, Materials for oral delivery of proteins and peptides. *Nat. Rev. Mater.* **5**, 127–148 (2020).
15. O. Eriksson, Evolution of angiosperm seed disperser mutualisms: The timing of origins and their consequences for coevolutionary interactions between angiosperms and frugivores. *Biol. Rev. Camb. Philos. Soc.* **91**, 168–186 (2016).
16. K. C. Kwon, R. Nityanandam, J. S. New, H. Daniell, Oral delivery of bioencapsulated exendin-4 expressed in chloroplasts lowers blood glucose level in mice and stimulates insulin secretion in beta-TC6 cells. *Plant Biotechnol. J.* **11**, 77–86 (2013).
17. A. Sherman *et al.*, Suppression of inhibitor formation against factor VIII in hemophilia A mice by oral delivery of antigens bioencapsulated in plant cells. *Blood* **124**, 1659–1668 (2014).
18. J. C. Espín, M. T. García-Conesa, F. A. Tomás-Barberán, Nutraceuticals: Facts and fiction. *Phytochemistry* **68**, 2986–3008 (2007).
19. P. A. Tsuji, K. K. Stephenson, K. L. Wade, H. Liu, J. W. Fahey, Structure-activity analysis of flavonoids: Direct and indirect antioxidant, and antiinflammatory potencies and toxicities. *Nutr. Cancer* **65**, 1014–1025 (2013).
20. N. Khan, D. N. Syed, H. C. Pal, H. Mukhtar, F. Afaq, Pomegranate fruit extract inhibits UVB-induced inflammation and proliferation by modulating NF-κB and MAPK signaling pathways in mouse skin. *Photochem. Photobiol.* **88**, 1126–1134 (2012).
21. N. G. Lamson, R. L. Ball, K. C. Fein, K. A. Whitehead, Thrifty, rapid intestinal monolayers (TRIM) Using Caco-2 epithelial cells for oral drug delivery experiments. *Pharm. Res.* **36**, 172 (2019).
22. K. Whitehead, N. Karr, S. Mitragotri, Safe and effective permeation enhancers for oral drug delivery. *Pharm. Res.* **25**, 1782–1788 (2008).
23. N. G. Lamson, G. Cusimano, K. Suri, A. Zhang, K. A. Whitehead, The pH of piperazine derivative solutions predicts their utility as transepithelial permeation enhancers. *Mol. Pharm.* **13**, 578–585 (2016).
24. L. Pastorelli, C. De Salvo, J. R. Mercado, M. Vecchi, T. T. Pizarro, Central role of the gut epithelial barrier in the pathogenesis of chronic intestinal inflammation: Lessons learned from animal models and human genetics. *Front. Immunol.* **4**, 280 (2013).
25. A. Kosińska-Cagnazzo, S. Diering, D. Prim, W. Andlauer, Identification of bioaccessible and uptaken phenolic compounds from strawberry fruits in in vitro digestion/Caco-2 absorption model. *Food Chem.* **170**, 288–294 (2015).
26. R. Tsao, R. Yang, Optimization of a new mobile phase to know the complex and real polyphenolic composition: Towards a total phenolic index using high-performance liquid chromatography. *J. Chromatogr. A* **1018**, 29–40 (2003).
27. Y. Lin *et al.*, Comparative transcriptome profiling analysis of red- and white-fleshed strawberry (Fragaria × ananassa) provides new insight into the regulation of the anthocyanin pathway. *Plant Cell Physiol.* **59**, 1844–1859 (2018).
28. C. Li, J. D. Trombley, M. A. Schmidt, A. E. Hagerman, Preparation of an acid butanol standard from fresh apples. *J. Chem. Ecol.* **36**, 453–460 (2010).
29. N. P. Seeram, R. Lee, H. S. Scheuller, D. Heber, Identification of phenolic compounds in strawberries by liquid chromatography electrospray ionization mass spectroscopy. *Food Chem.* **97**, 1–11 (2006).
30. F. Giampieri *et al.*, The strawberry: Composition, nutritional quality, and impact on human health. *Nutrition* **28**, 9–19 (2012).
31. S. Tuvia *et al.*, A novel suspension formulation enhances intestinal absorption of macromolecules via transient and reversible transport mechanisms. *Pharm. Res.* **31**, 2010–2021 (2014).
32. D. J. Brayden, S. Maher, Transient permeation enhancer® (TPE®) technology for oral delivery of octreotide: A technological evaluation. *Expert Opin. Drug Deliv.* **18**, 1501–1512 (2021).
33. A. Banerjee *et al.*, Ionic liquids for oral insulin delivery. *Proc. Natl. Acad. Sci. U.S.A.* **115**, 7296–7301 (2018).
34. N. G. Lamson, A. Berger, K. C. Fein, K. A. Whitehead, Anionic nanoparticles enable the oral delivery of proteins by enhancing intestinal permeability. *Nat. Biomed. Eng.* **4**, 84–96 (2020).

35. A. Banerjee, J. Lee, S. Mitragotri, Intestinal mucoadhesive devices for oral delivery of insulin. *Bioeng. Transl. Med.* **1**, 338–346 (2016).
36. S. Tsukita, M. Furuse, M. Itoh, Multifunctional strands in tight junctions. *Nat. Rev. Mol. Cell Biol.* **2**, 285–293 (2001).
37. M. Z. Gilcrease, Integrin signaling in epithelial cells. *Cancer Lett.* **247**, 1–25 (2007).
38. A. Taverner *et al.*, Enhanced paracellular transport of insulin can be achieved via transient induction of myosin light chain phosphorylation. *J. Control. Release* **210**, 189–197 (2015).
39. F. McCartney, J. P. Gleeson, D. J. Brayden, Safety concerns over the use of intestinal permeation enhancers: A mini-review. *Tissue Barriers* **4**, e1176822 (2016).
40. P. S. Lim, Y. K. Chang, T. K. Wu, Serum lipopolysaccharide-binding protein is associated with chronic inflammation and metabolic syndrome in hemodialysis patients. *Blood Purif.* **47**, 28–36 (2019).
41. E. Lau *et al.*, The role of I-FABP as a biomarker of intestinal barrier dysfunction driven by gut microbiota changes in obesity. *Nutr. Metab. (Lond.)* **13**, 31 (2016).
42. J. P. M. Derikx, D. H. S. M. Schellekens, S. Acosta, Serological markers for human intestinal ischemia: A systematic review. *Best Pract. Res. Clin. Gastroenterol.* **31**, 69–74 (2017).
43. C. M. Van Itallie, J. M. Anderson, Claudins and epithelial paracellular transport. *Annu. Rev. Physiol.* **68**, 403–429 (2006).
44. J. M. Anderson, C. M. Van Itallie, Physiology and function of the tight junction. *Cold Spring Harb. Perspect. Biol.* **1**, a002584 (2009).